Proceedings of CONF-MSS 2026 Symposium: Advanced Composite Materials and Polymer Chemistry
DOI: 10.54254/2755-2721/2026.AD33215

The Influences of Maximum Thickness on the Aerodynamic Characteristics of Airfoils at High Reynolds Numbers

Zehan Chai

Chang'an Dublin International College of Transportation, Chang'an University, Xi'an, China
2023902470@chd.edu.cn

Abstract. This paper presents a numerical study analyzing the influences of maximum thickness on the aerodynamic characteristics of airfoils under high Reynolds number conditions (Re = 2.2×10^6). The NACA2408, NACA2410 and NACA2412 airfoils, each with identical camber and camber position but maximum thicknesses of 8%, 10% and 12% respectively, were selected as the subjects of this study. Two-dimensional steady-state numerical simulations were conducted in a computational fluid dynamics (CFD) environment. The aerodynamic performance was evaluated over an angle of attack (AoA) range of 0° to 12°, while the evolution of flow field structures was analyzed using pressure and velocity contour plots. The results indicate that the lift coefficients of the three airfoils increase approximately linearly with AoA, whilst the drag coefficients show a more pronounced increase at high AoA. The lift-to-drag ratio peaks at around 8°, indicating optimal aerodynamic efficiency. The influence of thickness on aerodynamic performance is AoA dependent: thinner airfoils exhibit slightly better efficiency at moderate AoA, whereas airfoils of moderate thickness demonstrate superior overall performance at higher AoA. These findings provide a reference for optimising airfoil thickness parameters under high Reynolds number conditions.

Keywords: High Reynolds number, numerical simulations, aerodynamic characteristics

1. Introduction

An airfoil is a common cross-section of an aircraft wing, the functions of an airfoil are to provide lift under the influence of the incoming airstream and to reduce drag to a minimum. Nevertheless, no such thing as a universal best solution exists to the airfoils since other missions and conditions of operation demand other aerodynamic trade-offs. Since aerodynamic performance must involve a trade-off between lift and drag, any alteration in the geometric parameters of the airfoil will impact directly on the performance of the aircraft and on the operating conditions in which it can be used [1,2].

NACA series of airfoils are employed across many studies of the aerodynamic behavior of airfoils because of its descriptive naming scheme and the ability to control its geometry. The earlier works have shown that in the four-digit NACA airfoil nomenclature, the first two numbers, and the final two numbers are most significant geometric properties of the airfoil, including the maximum curvature, the location of maximum curvature, and the maximum thickness, respectively. In turn, the

© 2026 The Authors. This is an open access article distributed under the terms of the Creative Commons Attribution License 4.0 (https://creativecommons.org/licenses/by/4.0/).

DOI: 10.54254/2755-2721/2026.AD33215

choice of NACA2408, NACA2410 and NACA2412 as the focus of the present research is a definite plus in terms of controlled variables: all three have the same max thickness, same max curvature and same position of max curvature, and they are members of the 24xx family, with the only significant difference being the max thickness they have, which are 8, This geometry enables a closer study on how changes in maximum thickness can affect the aerodynamic properties of the airfoils, whilst limiting the effects of other geometric variables.

Aerodynamic performance of airfoils has been studied in the past years with much attention paid to changes in angle of attack (AoA), comparison of airfoil designs and local geometric changes to enhance lift and decrease drag. A computational fluid dynamics (CFD) comparison of the NACA0012 and NACA4418 airfoils was performed by Mahato et al. where asymmetric airfoils showed better overall aerodynamic performance at certain conditions of operation [3]. Rayhan et al. performed numerical studies on NACA 4412 with slots and grooves, and found out that local modifications could delay the flow separation and increase the stall AoA [4]. Gong conducted two-dimensional CFD simulations of the NACA 2412 and NACA 0012 at Re 2.2 x 10 6 and found that various airfoils have varying strengths in lift-to-drag behavior over different angles-of-attack [5]. Moreover, other researchers have also done research based on other perspectives such as leading-edge corrugation, serrated Gurney flaps, airfoil optimization, multi-criteria evaluation and aerodynamic optimization under special flight conditions and hence contributed more to the research material on the regulation and optimization of airfoil aerodynamic performance [6-10]. In general, the research that has been conducted so far has mainly revolved around variation in airfoil types, variation in AoA, local flow control or optimization of multi parameters. None of the studies have, however, systematically shown how the maximum thickness as a single variable can affect the aerodynamic properties of airfoils at large Reynolds numbers, whilst keeping consistent the maximum curvature and its location.

Against this background, this paper investigates how the maximum thickness of an airfoil influences its aerodynamic performance at high Reynolds numbers. Under uniform flow conditions and numerical settings, the paper will compare the pressure and velocity distributions of three airfoils with small, medium, and large AoA. It particularly examines the variation of the relevant parameters with AoA, and further explains how variations in maximum thickness affect separation patterns and development of boundary layers, resulting in higher drag, alterations in aerodynamic efficiency, and variations in potential stall properties, and thus forms a basis of selecting airfoil thickness in high Reynolds number situations.

2. Numerical model

2.1. Geometric models and computational domains

The geometric models of NACA2408, NACA2410, and NACA2412 are shown in Figure 1. Figure 2 shows the computational region adopted in the numerical simulation, which is defined as 15 times the chord length. The inlet is a velocity inlet and the outlet is a pressure outlet.

DOI: 10.54254/2755-2721/2026.AD33215

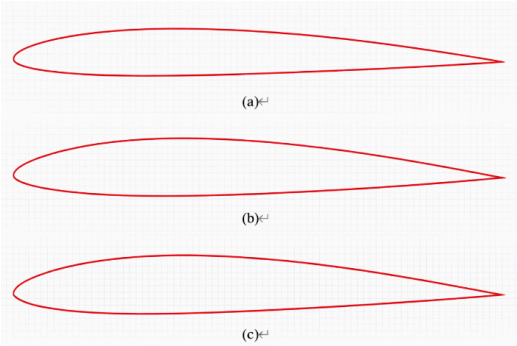

Figure 1. Geometric models of three different airfoils: (a) NACA2408; (b) NACA2410; (c) NACA2412. (picture credit : original)

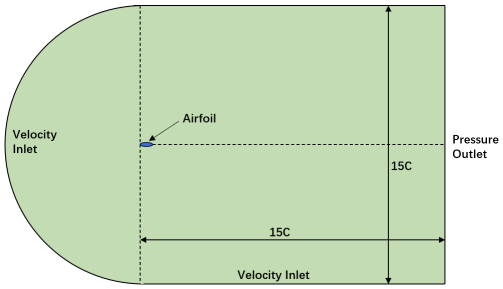

Figure 2. Computational domain. (picture credit : original)

2.2. Grid partitioning

This study employs a two-dimensional "C"-shaped computational domain and generates a two-dimensional structured mesh for solving the flow field. To facilitate control of mesh density in different regions and better capture flow characteristics, the entire computational domain is divided into six subregions for mesh generation. The outer region is discretized using coarser elements with a side length of approximately 0.4 m to improve computational efficiency and reduce computational costs while ensuring basic accuracy; In the vicinity of the airfoil, the mesh is locally refined with a minimum element size of 3×10^{-4} m to more accurately capture the velocity gradients and boundary layer variations near the airfoil surface. The overall mesh distribution is shown in Figure 3, the local details of the refined region around the airfoil are shown in Figure 4, and the local details of the innermost mesh layer are shown in Figure 5.

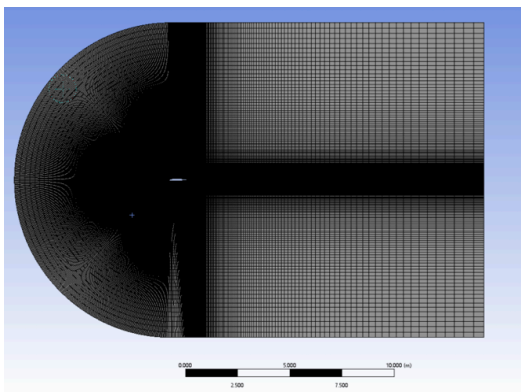

Figure 3. Computational domain grid. (picture credit: original)

DOI: 10.54254/2755-2721/2026.AD33215

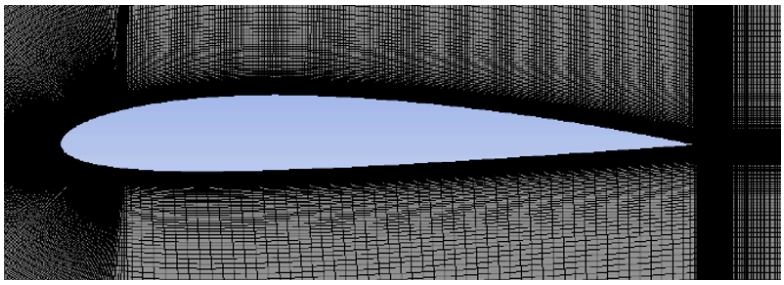

Figure 4. Detailed view of the local mesh around the airfoil. (picture credit: original)

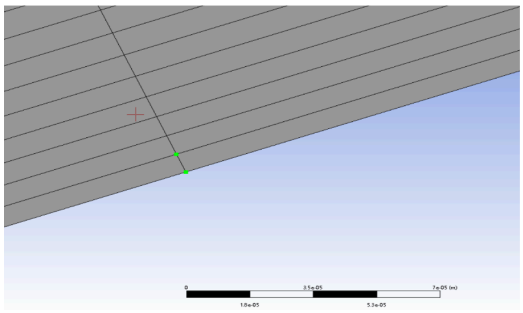

Figure 5. Detail of the innermost mesh. (picture credit: original)

2.3. Boundary conditions and control equations

Numerical calculations were performed using a pressure-based solver, with the k-ω SST turbulence model selected. A second-order upwind scheme was used for the convection term, and the Coupled algorithm was employed for the pressure-velocity coupling. Table 1 illustrates the boundary conditions of the simulation.

Table 1. Boundary conditions

Parameters	Values
Density (kg/m$^{3)}$	1.225
Viscosity (Pa·s)	1.7894×10^{-5}
Turbulence ratio	0.1
Turbulence scale	0.3
Inlet Velocity (m/s)	33
Reynolds Number	2.2×10^{6}

The fundamental control equations employed in the study are the incompressible continuity equation and the Navier-Stokes (N-S) equations, the expression for the first equation is shown in Equation (1).

$$\frac{\partial \rho}{\partial t} + \frac{\partial \rho u}{\partial x} + \frac{\partial \rho v}{\partial y} + \frac{\partial \rho w}{\partial z} = 0 \tag{1}$$

Where ρ represents the fluid density; u, v, and w represent the velocity components in different directions.

The N-S equations are given by Equation (2).

DOI: 10.54254/2755-2721/2026.AD33215

$$\rho\left(\frac{\partial \mathbf{u}}{\partial t}+\mathbf{u}\cdot\nabla\mathbf{u}\right)=-\nabla p+\nabla\cdot\left[(\mu+\mu_t)\left(\nabla\mathbf{u}+(\nabla\mathbf{u})^T\right)\right] \tag{2}$$

Where $\mathbf{u}$ is the velocity vector, p is the pressure, μ is the kinematic viscosity, and μ_t is the turbulent viscosity.

This study uses lift and drag coefficients to evaluate the aerodynamic performance of airfoils. The expressions are shown in Equations (3) and (4).

$$C_l=\frac{F_l}{1/2\rho V^2 A} \tag{3}$$

$$C_d=\frac{F_d}{1/2\rho V^2 A} \tag{4}$$

Where F_l represents the lift acting on the airfoil, F_d represents the drag acting on the airfoil, V represents the flow velocity, and A represents the reference area.

3. Results and discussion

This paper presents CFD simulations of three airfoil profiles with different maximum thicknesses namely NACA2408, NACA2410 and NACA2412. It examines the variation in the aerodynamic characteristics and distribution patterns of surface pressures and the velocity distributions across the airfoils between an AoA range of 0°–12° at high Reynolds numbers (Re = 2.2 × 10^6) and therefore examines the effects of maximum thickness on the lift, drag and aerodynamic efficiency.

3.1. The effect of different maximum thicknesses on C_l / C_d ratio

Figure 6 shows the variation in C_l / C_d ratio for the three airfoils at various AoA. It is clear that the C_l / C_d ratios of all three airfoil profiles rise significantly with increasing AoA, reaching a maximum near 8°, indicating that this AoA represents the optimal aerodynamic efficiency range for this operating condition. Among them, the NACA2408 with a thickness of 8% achieves the highest C_l / C_d ratio at 8°, suggesting that thinner airfoil profiles have certain efficiency advantages at moderate angles of attack. When the AoA increases to 12°, the C_l / C_d ratios of all three airfoils decrease; however, the NACA2410 with a thickness of 10% maintains a relatively high lift to drag ratio, demonstrating better overall behaviour. In general, the influence of maximum thickness on the C_l / C_d ratio is AoA sensitive: thinner airfoils are more efficient over the moderate AoA interval, whereas airfoils with a moderate thickness advantage is at the higher AoA.

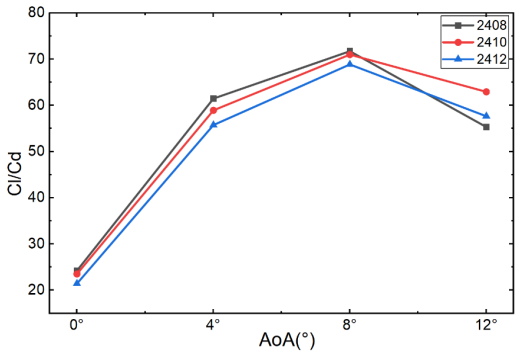

Figure 6. Variation curves of C_l / C_d ratio for airfoils with different maximum thicknesses under different AoA. (picture credit : original)

DOI: 10.54254/2755-2721/2026.AD33215

3.2. Patterns of change in lift and drag coefficients

Figure 7 indicates that for all three airfoil profiles, the lift coefficient C_l rises almost linearly as the AoA rises between 0° and 12°, showing that an increase in AoA causes an rise in the difference between the pressure in the upper and lower surfaces of the airfoil, thereby continuously increasing lift. Meanwhile, the drag coefficient C_d also increases with increasing AoA, with a more pronounced increase at higher angles of attack (such as 12°), indicating that flow separation tends to intensify and the wake thickens at high angles of attack, leading to a rapid increase in drag. A comparison of different airfoil thicknesses reveals that the differences in C_l and C_d among the three airfoils are relatively small within the low-too-medium angle-of-attack range; however, these differences become more pronounced at 12°, with the NACA2410 exhibiting a relatively lower C_d and higher C_l, demonstrating its superior overall aerodynamic performance at larger AoA.

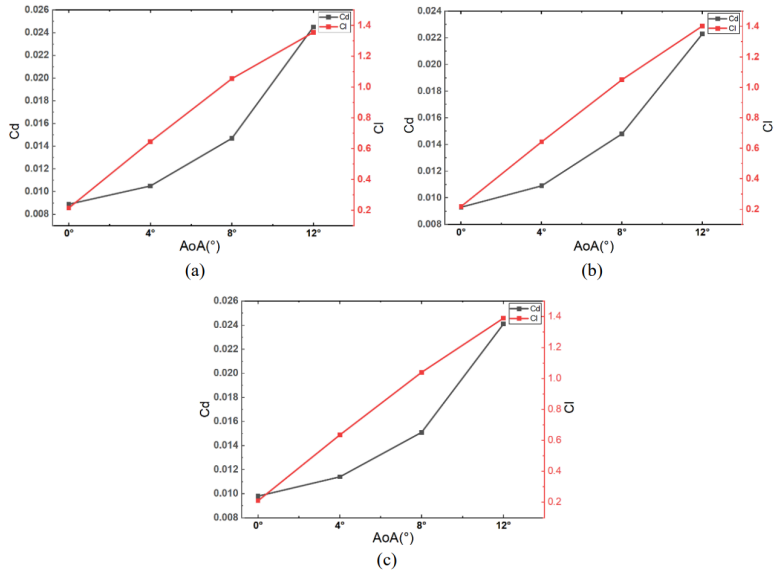

Figure 7. Curves of C_l / C_d ratio for the three airfoil profiles under different AoA: (a) NACA 2408; (b) NACA 2410; (c) NACA 2412. (picture credit : original)

3.3. Analysis of pressure and velocity distribution characteristics of airfoils

Since the pressure and velocity distributions of the NACA2408, NACA2410, and NACA2412 airfoils exhibit similar overall patterns at the same AoA with only slight variations in intensity and range, the NACA2410 has been selected as a representative example for presentation and analysis.

As illustrated in Figure 8, as the AoA increases from 0° to 12°, the low-pressure region on the upper airfoil surface grows steadily and towards the leading edge, while the high-pressure region on the lower surface expands relatively. This causes the pressure difference between different surfaces to increase continuously, leading to an increase in C_l as the AoA increases. In the low AoA range (0°–4°), the pressure distribution is relatively smooth; however, when the AoA increases to 8° and 12°, the suction peak on the upper surface becomes significantly stronger, and the adverse pressure gradient intensifies, creating conditions for flow separation. This also explains the rapid increase in drag at high angles of attack.

As illustrated in Figure 9, with increasing AoA, the acceleration region over the upper surface of the airfoil enlarges and the peak flow velocity rises, indicating that the flow acceleration effect intensifies. At the same time, the wake region gradually thickens, and the area of the low-speed

DOI: 10.54254/2755-2721/2026.AD33215

region increases significantly. This is particularly evident at the 12° AoA, where the wake extends more noticeably, suggesting increased flow losses and the potential for local separation. This trend of wake thickening and low-speed region expansion is consistent with the variation in C_d as the AoA increases.

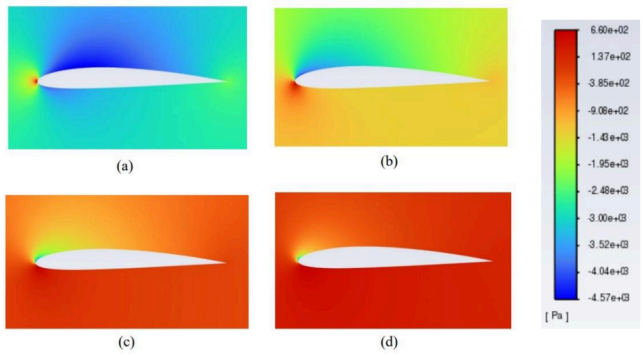

Figure 8. Pressure contour plots for the NACA 2410 airfoil: (a) 0°; (b) 4°; (c) 8°; (d) 12°. (picture credit : original)

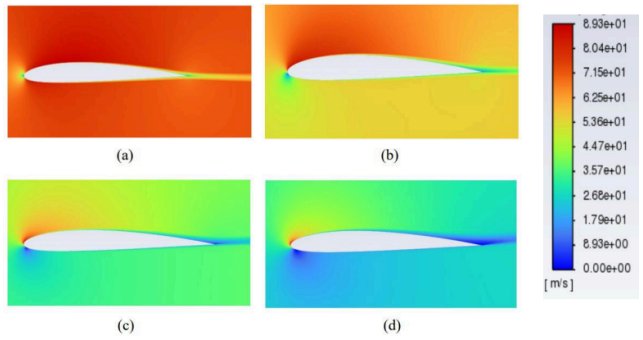

Figure 9. Velocity contour plots for the NACA 2410 airfoil: (a) 0°; (b) 4°; (c) 8°; (d) 12°. (picture credit : original)

4. Conclusion

This paper provides a comparative investigation of the aerodynamic behaviour of three airfoil profiles with different maximum thicknesses—NACA2408, NACA2410, and NACA2412—using CFD simulation software. The study analyzed the lift and drag characteristics, as well as the pressure/ velocity distributions within the AoA range of 0°–12°, and investigated the effects of variations in maximum thickness on the aerodynamic behaviour of the airfoils. The main conclusions of this paper are as follows:

(1). As the AoA increases from 0° to 12°, the lift coefficient C_l of all three airfoil profiles continues to increase, while the drag coefficient C_d rises in tandem; the increase in drag is more pronounced at higher AoA.

(2). The C_l / C_d ratios of all three airfoil profiles peaks at around 8°, indicating that this AoA represents the high-efficiency operating range under these conditions; When the AoA increases to 12°, the C_l / C_d ratio decreases due to the faster growth in drag.

(3). The effect of maximum thickness on aerodynamic behaviour is AoA dependent: the differences among the three airfoils are small at low and medium AoA; at 12°, the NACA2410 exhibits higher lift and lower drag, resulting in relatively superior overall aerodynamic efficiency.

DOI: 10.54254/2755-2721/2026.AD33215

References

[1] Soetanto, M.F., Sugianto, H.B. and Zuhri, M.R. (2023) Numerical study of aerodynamic characteristics of airflow around NACA 0012 and NACA 4412 airfoils at Re = 170000, International Journal of Applied Technology Research, 4(2), 133–146.
[2] Dhakal, S., Bhattarai, K.R. and Sanjay, M. (2023) Computational analysis of the aerodynamic performance of NACA 4412 and NACA 23012 airfoils, International Research Journal of Engineering and Technology (IRJET), 10(12), 265–273.
[3] Mahato, A., Singh, R.K., Barnwal, R. and Rana, S.C. (2023) Aerodynamic characteristics of NACA 0012 vs. NACA 4418 airfoil for wind turbine applications throughCFDsimulation, Materials Today: Proceedings. 74, 1539–1546, Elsevier, Amsterdam, Netherlands.
[4] Rayhan, A.M., Hossain, M.S., Mim, R.H. and Ali, M. (2024) Computational and experimental study on the aerodynamic performance of NACA 4412 airfoil with slot and groove, Heliyon, 10(11), e31595.
[5] Gong, Z. (2025) CFD Analysis of NACA2412 and NACA0012 at Low Reynolds (2.2×10^6) Numbers Based on ANSYS Fluent, Applied and Computational Engineering, 127, 59–67.
[6] Chen, W., Qiao, W. and Wei, Z. (2020) Aerodynamic performance and wake development of airfoils with wavy leading edges, Aerospace Science and Technology, 106, 106216.
[7] Ye, X., Hu, J., Zheng, N. and Li, C. (2023) Numerical study on aerodynamic performance and noise of wind turbine airfoils with serrated gurney flap, Energy, 262(Part B), 125574.
[8] Zhang, J., Wang, H., Tian, W. and Deng, X. (2023) Optimizing Airfoil Aerodynamic Characteristics by Using Proposed CSA-KJ Method', Applied Sciences, 13(2), 924.
[9] Seyhan, M., Es, H.A. and Sarioglu, M. (2024) Overall aerodynamic performance of the airfoils with different amplitudes via a fuzzy decision making based Taguchi methodology, Applied Soft Computing, 165, 112057.
[10] Aprovitola, A., Iuspa, L., Pezzella, G. and Viviani, A. (2023) Aerodynamic optimization of airfoils shape for atmospheric flight on Mars planet, Acta Astronautica, 212, 580–594.